Journal of Magnetics 8(1), 32-35 (2003)

Temperature Dependence of Exchange Coupling on Magnetic Tunnel Junctions

Yongkang Hu[1], CheolGi Kim*[1], Tomasz Stobiecki[2], Chong-Oh Kim[1] and Kimin Hong[3]

[1]*Department of Materials Engineering, Chungnam National University, Daejeon 305-764, Korea*
[2]*Department of Electronics, University of Mining and Metallurgy, 30-059 Krakow, Poland*
[3]*Department of Physics, Chungnam National University, Daejeon 305-764, Korea*

(Received 10 December 2002)

Magnetic Tunnel Junctions (MTJs) were fabricated on thermally oxidized Si (100) wafers using DC magnetron sputtering. The film structures were Ta(50 Å)/Cu(100 Å)/Ta(50 Å)/$Ni_{80}Fe_{20}$(20 Å)/Cu(50 Å)/$Mn_{75}Ir_{25}$(100 Å)/$Co_{70}Fe_{30}$(25 Å)/Al-O(15 Å)/$Co_{70}Fe_{30}$(25 Å)/$Ni_{80}Fe_{20}$(t)/Ta(50 Å), with t = 0 Å, 100 and 1000 Å, respectively. X-ray diffraction has shown improvement of (111) texture of $IrMn_3$ and Cu by annealing. The exchange-biased energy is almost inversely proportional to temperature. The difference between the coercivity H_c and the exchange biased field H_E for t = 0 Å sample is smaller than that for t = 1000 Å. For the pinned layer, the decreasing rate of the coercivity with the temperature is higher compared to that of the exchange field, but variation of H_c is similar to that of the exchange field for free layer.

Key words : TMR, XRD, exchange coupling

1. Introduction

The MTJs are structures comprising two ferromagnetic layers separated by an ultra-thin insulating barrier layer (FM/I/FM). Recently large MR ratio at room temperature has been reported [1-2], which makes MTJs promising candidates for magnetic random access memory (MRAM) devices [3] and read heads in hard disk drivers [4]. For applications to MRAM device and read heads, exchange coupling is one of the most important factors contributing to the reversal magnetization of two magnetic layers. The interfacial exchange coupling between antiferromagnetic (AF) layer and ferromagnetic (FM) layer causes a shift, H_E, of the hysteresis loop in the field direction as well as the enhancement of coercivity, H_C. H_E decreases as temperature is increased and becomes zero at a certain temperature, so called "block temperature" [5]. Although there have been numerous attempts to explain this phenomenon [6], the origin of the exchange coupling with the temperature dependence has not yet been fully understood.

The interlayer exchange coupling between free layer and pinned-FM layer dominates the characteristics of MR loop at low fields. Interlayer exchange coupling is explained in two ways; one is the RKKY-like coupling through an indirect exchange mediated by the itinerant electrons [7]. The other is Neel's orange peel coupling from magnetic dipole interaction related to interfacial morphological corrugations [8-10]. However, an insulating layer prevents electron itinerancy reducing RKKY interaction, orange peel coupling seems to be more plausible for explanation of the exchange coupling.

In this paper, the MR loop was measured under both high field and low field ranges to investigate the temperature dependence of exchange field, coercivity, and exchange biased energy.

2. Experimental

The magnetic tunneling junctions (MTJs) with the structure Ta(50 Å)/Cu(100 Å)/Ta(50)/$Ni_{80}Fe_{20}$(20 Å)/Cu (50 Å)/$Mn_{75}Ir_{25}$(100 Å)/$Co_{70}Fe_{30}$(25 Å)/Al-O(15 Å)/$Co_{70}Fe_{30}$(25 Å)/$Ni_{80}Fe_{20}$(t)/Ta(50 Å), with t = 0 Å, 100 Å, and 1000 Å (Fig. 1), were fabricated on the oxidized silicon by the DC sputtering system with a base pressure: 3×10^{-9} Torr. For barrier formation, a 15 Å thickness metallic Al film was deposited and subsequently oxidized in an oxidation chamber with a radial line slot antennal (RLSA) operating at 2.45 GHz microwaves [11]. A gas mixture of oxygen and Kr was introduced for the plasma oxidation. The junction samples with t = 100 Å were

*Corresponding author: Tel: +82-42-821-6229, e-mail: cgkim@cnu.ac.kr

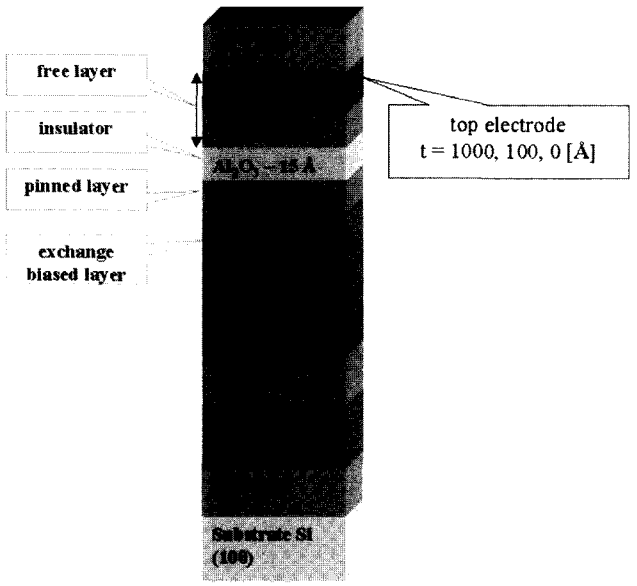

Fig. 1. Multilayer structure of MTJ.

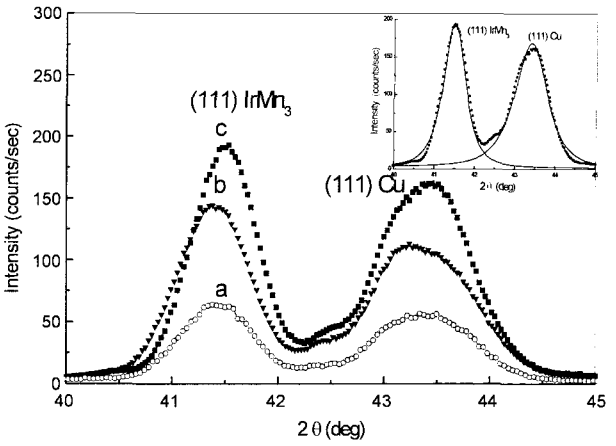

Fig. 2. Textured part of θ-2θ scan with fcc-(111)$IrMn_3$ and (111)Cu planes for as-deposited samples with (a) free layer of $Co_{70}Fe_{30}$(25 Å), (b) $Co_{70}Fe_{30}$(25 Å)/$Ni_{80}Fe_{20}$(t = 100 Å) and (c) free layer of $Co_{70}Fe_{30}$(25 Å)/$Ni_{80}Fe_{20}$(t = 100 Å) annealed at 200 °C. Inset figure in fitting lines of fcc-(111)$IrMn_3$ and (111)Cu peaks.

thermally annealed at 200 °C in a magnetic field of 1 kOe, followed by field cooling. For the sake of diffraction measurements, identical structures were fabricated on a 10 mm disk along with the samples.

The MR ratio of t = 1000 Å sample, field-annealed at 270 °C, was measured at temperatures between 30 K and 300 K by using the four-probe method at low field of ~50 Oe and at high field of ~4 kOe, respectively. Magnetization curves and hysteresis loops were obtained using vibrating sample magnetometer (VSM) at room temperature and a superconducting quantum interference device (SQUID) magnetometer at low temperatures.

3. Results and Discussion

3.1. Film Microstructure

Figure 2 shows high angle X-ray diffraction profiles of the as-desposited and annealed samples. Thickness of $Ni_{80}Fe_{20}$ was 0 Å and 100 Å, respectively. The high peaks around $2\theta = 41°$~$42°$ results from diffraction caused by (111) of $IrMn_3$. The broad peaks around $2\theta = 43°$~$44°$ correspond to the diffraction from Cu (111) (not distinguish with the fcc (111) texture of $Ni_{80}Fe_{20}$ and $Co_{70}Fe_{30}$). Compared curve (b) with curve (c), curve (c) shows higher peaks and a slight shift of location after the anneal in vacuum at 200 °C. The peak ratio of (111)$IrMn_3$/(111)Cu decreases from 1.27 before annealing to 1.18 after annealing. It indicates improvements in crystallinity of the multiplayer structure [12-13]. The layer structure is consistent with the fit to the experimental curves shown in the inset of Fig. 2. Lattice planes and lattice constants were determined from the peak positions. The parameters for the sample with the thickness t = 100 Å have changed from (111)$IrMn_3$ d = 2.181 Å (a = 3.777 Å) and Cu d = 2.087 Å (a = 3.614 Å) before annealing to (111)$IrMn_3$ d = 2.176 Å (a = 3.768 Å) and Cu d=2.084 Å (a = 3.610 Å) after annealing.

3.2. Exchange coupling of pinned layer

Figure 3 shows the hysteresis loops of t = 0 Å sample annealed at 200 °C as a function of temperatures from 10 K to 300 K using a SQUID. From these loops, we could get the exchange-biased field, H_E, of pinned-FM layer. The exchange-biased energy E_{EB} was calculated by using the formula of $E_{EB} = \mu_0 M_s H_E t_p$, where M_s and t_p are

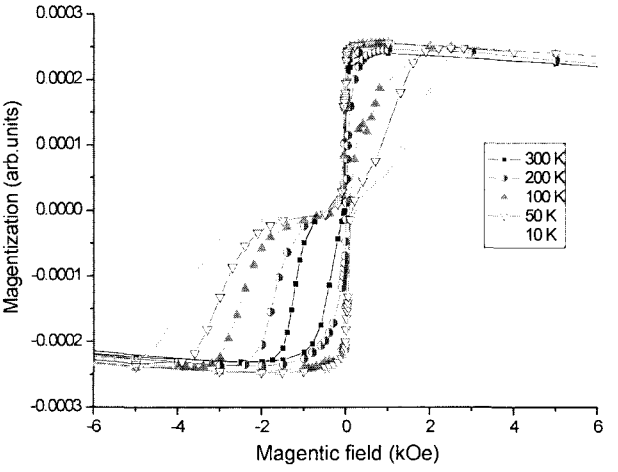

Fig. 3. Hysteresis loop of annealed sample at 200 °C with the t = 0 Å as a function of temperature.

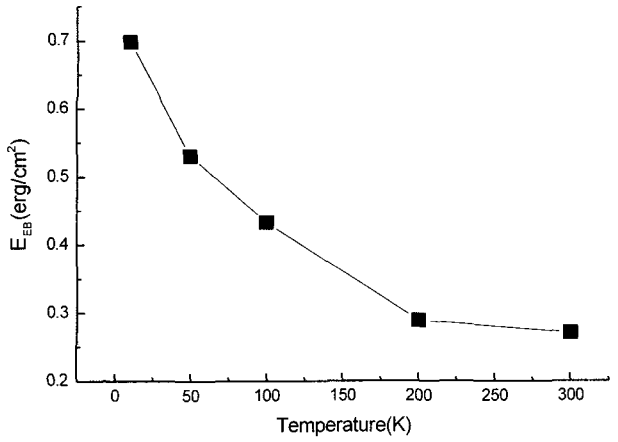

Fig. 4. Exchange-biased energy as a function of temperature for annealed sample with $t = 0$ Å.

saturation magnetization and thickness of pinned layer, respectively. The temperature dependence of the exchange-biased energy is shown in Fig. 4.

It can be seen that the exchange-biased energy is almost inversely proportional to temperature. Fig. 3 exhibits the change of the magnetization at different temperatures. As the temperature decreases, the magnetization almost did not change. And the decrease of E_{EB} as the temperature increases mainly depends on weakening of exchange-biased field H_E. The major MR loop was characterized by the magnetic behavior of the magnetically hard electrode of $Co_{70}Fe_{30}$ (25 Å) pinned by the exchange biased coupling of antiferromagentic $Mn_{75}Ir_{25}$ (100 Å) layer, or so called "pinned layer". Fig. 5 shows the MR loop at room temperature under high fields of ~4 kOe obtained from the $t = 1000$ Å sample with the tunneling junction size of 250×250 μm^2 after annealing. Exchange biased field,

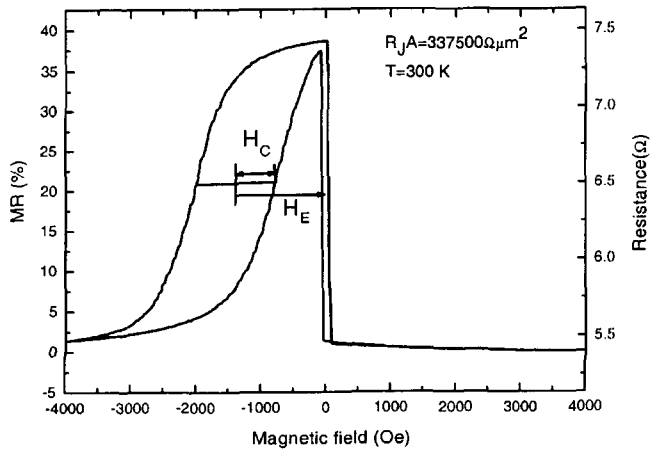

Fig. 5. MR loop of the $t = 1000$ Å sample with the junction size of 250×250 μm^2 at room temperature.

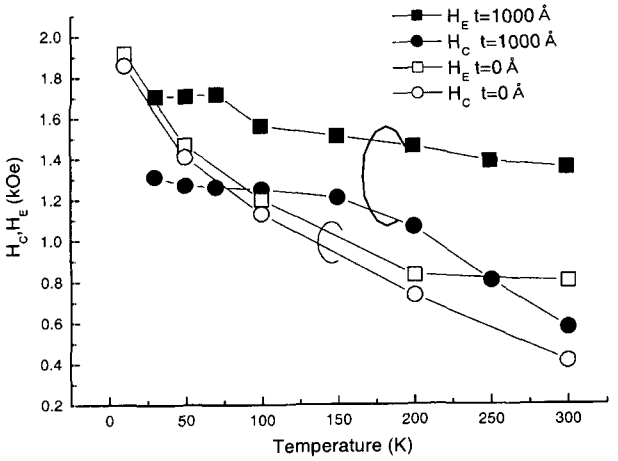

Fig. 6. Temperature dependence of exchange field and coercivity of pinned layer for the annealed sample with $t = 1000$ Å, 0 Å.

H_E, and coercivity, H_C, were evaluated from the MR loop, as marked in this figure. The achievement of high MR ratio of 38.67% is due to the improved interface between FM/I/FM layers after annealing, as indicated by XRD, and the reduction of the defect density in the Al_2O_3 barrier after annealing. The exchange-biased field of $H_E = 1440$ Oe corresponds to exchange biased energy of 0.52 erg/cm^2 [14].

Figure 6 shows the temperature dependence of exchange-biased field and coercivity of the pinned layer of the annealed sample, evaluated from MR loops. The H_E and H_c decrease rapidly with the increase of the temperature. The reason is that the temperature dependence of magnetization in the pinned layer depends on the thermal instabilities of antiferromagnetic state in antiferromagnetic grains, much as occurs in superparamagnetic grains. It is thought that the antiferromagnetic state in the grain is stable and the unidirectional anisotropy causes large shift at low temperature. However, as the temperature increases, the antiferromagnetic state becomes unstable, due to the thermal excitation over energy barriers [6] and the exchange field is reduced. Comparing with the results by SQUID measurements of the $t = 0$ Å sample, we can see a clear difference in coercivity and exchange-biased field of the pinned layer with $t = 1000$ Å. It might be resulting from NiFe effect of the free layer.

3.3. Exchange coupling of free layer

Fig. 7 shows the temperature dependence of minor MR loops for annealed sample with $t = 1000$ Å, where exchange change field, H_E, and coercivity, H_C, were evaluated from the MR loop, as marked in the figure. The coercivity of the free layer is about 3 Oe and the minor MR loop is

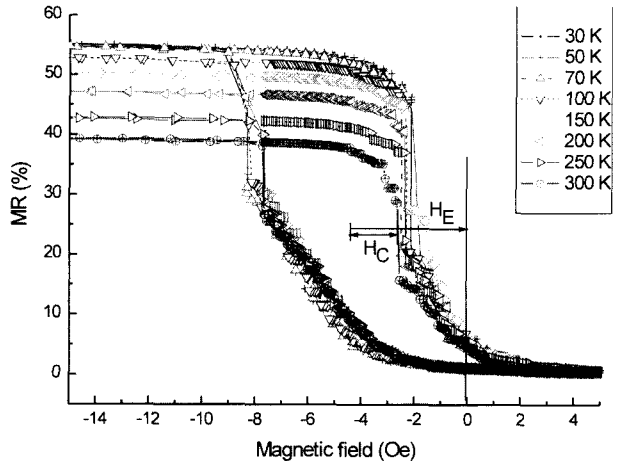

Fig. 7. Minor MR loops as a function of temperature for the annealed sample with $t = 1000$ Å.

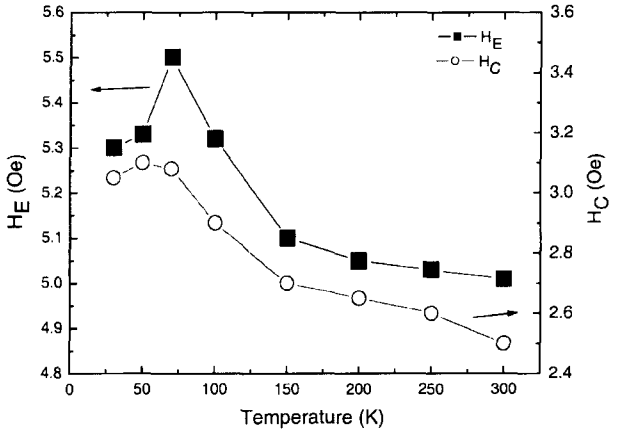

Fig. 8. Temperature dependence of exchange field and coercivity of free layer for the annealed sample with $t = 1000$ Å.

shift to about 5 Oe from zero magnetic field at room temperature. Fig. 8 shows the temperature dependence of exchange field and coercivity of free layer. It can be seen that exchange field, H_E, of free layer are higher than coercivity, H_C. Exchange field and coercivity decrease with increasing temperature from 30 K to 300 K. The decreasing rate of coercivity of the free layer is similar to that of exchange field, indicating the same mechanism may be involved in H_E and enhanced H_C.

4. Conclusion

The X-ray analysis reveals that annealing treatment has improved the crystallinity and texture of the sample. Appropriate annealing induces high exchange biased energy and MR ratio and strengthens the interaction of the exchange biased coupling. MR ratio, resistance, exchange field, coercivity and exchange-biased energy increase with decreasing temperature, and exchange-biased energy mainly depends on the exchange-biased field.

References

[1] T. Miyazaki and N. Tezuka, J. Magn. Magn. Mater. **139**, L231 (1995).
[2] J. S. Moodera, L. R. Kinder, T. M. Wong, and R. Meservey, Phys. Rev. Lett. **74**, 3273 (1995).
[3] S. S. P. Parkin, K. P. Roche, M. G. Samant, P. M. Rice, R. B. Beyers, R. E. Scheuerlein, E. J. O'Sullivan, S. L. Brown, J.Bucchigano, D. W. Abraham, Yu Lu, M. Rooks, P. L. Trouilloud, R. A. Waner, and W. J. Gallagher, J. Appl. Phys. **85**, 5828 (1999).
[4] R. Richter, L. Bär, J. Wecker, and G. Reiss, Appl. Phys. Lett. **80**, 1291 (2002).
[5] C. Tsang, N. Heiman, and K. Lee, J. Appl. Phys. **52**, 2471 (1981); C. Tsang and K. Lee, J. Appl. Phys. **53**, 2605 (1982).
[6] M. D. Stiiles and R. D. McMichael, Phys. Rev. B. **60**, 12950 (1999).
[7] M. A. Ruderman, C. Kittel, Phys. Rev. **96**, 99 (1954).
[8] L. Neel, C. R. Acad. Sci. **255**, 1676 (1962).
[9] C. Lee, J. A. Bain, S. Chu, and M. E. McHenry, J. Appl. Phys. **91**, 7113 (2002).
[10] F. Stobiecki, T. Stobiecki, B. Ocker, W. Maas, W. Powroznik, A. Paja, C. Loch, and K. Roell, Acta Phys. Polon. (A) **97**, 523 (2000).
[11] M. Tsunoda, K. Nishikawa, S. Ogata, and M. Takahashi, Appl. Phys. Lett. **80**, 3135 (2002).
[12] M. Tsunoda, Y. Tsuchiya, T. Hashimoto, and M. Takahashi, J. Appl. Phys. **87**, 4375 (2000).
[13] G. Anderson, Y. Huai, and L. Miloslawsky, J. Appl. Phys. **87**, 6989 (2000).
[14] M. Tsunoda, Y. Tsuchiya, T. Hashimoto, and M. Takahashi, J. Appl. Phys. **87**, 4375 (2000).